Scientia Iranica B (2023) 30(3), 953–968

SCIENTIA IRANICA

Sharif University of Technology
Scientia Iranica
Transactions B: Mechanical Engineering
http://scientiairanica.sharif.edu

Performance evaluation of a kalina cycle using a novel extended thermodynamic analysis

M. Akhoundi, P. Kazemiani-Najafabadi, and E. Amiri Rad*

Department of Mechanical Engineering, Center of Computational Energy, Hakim Sabzevari University, Sabzevar, Iran.

Received 21 July 2021; received in revised form 5 August 2022; accepted 31 October 2022

KEYWORDS
Extended thermodynamic analysis;
Advanced exergy analysis;
Conventional exergy analysis;
Kalina cycle;
Improvement priority.

Abstract. This research presents a novel Extended Thermodynamic Analysis Method (ETAM) to respond to the issue of 'which equipment holds the highest priority of receiving improvements in a thermodynamic cycle'. This novel analysis comprises three parts: extended energy, extended entropy, and extended exergy analyses. As a case study, a low-temperature geothermal Kalina cycle system-34 was analyzed. The results of Conventional Exergy Analysis Method (CEAM), Advanced Exergy Analysis Method (AEAM), and the proposed novel method were compared with each other. CEAM results indicate that the condenser, followed by the evaporator and turbine, has the most exergy destruction. In contrast, according to AEAM results, the top priority for improvement should be given to the condenser, followed by turbine and Low-Temperature Recuperator (LTR). The improvement priority using the presented novel extended analysis was also given to the condenser, turbine, and LTR, the finding being the same as the results of AEAM, while the proposed novel method is less complicated than the AEAM.

1. Introduction

Exergy is the maximum utility that can be achieved from a system in a given state in a defined environment [1]. The Conventional Exergy Analysis Method (CEAM) plays a crucial role in calculating the irreversibility of system components. Hatami et al. [2] investigated an indirect solar dryer. The outcomes of the energy and exergy evaluation point to higher stream exergy at a higher speed of air and lower irreversibility. Ghorbani et al. [3] studied a wind farm integrated with compressed air energy storage that uses phase change material. According to the results of energy and exergy analyses, exergy efficiency and round-trip efficiency reached 80.71% and 70.83%, respectively. Elhelw et al. [4] analyzed a 650 MW thermal power plant based on exergy analysis. According to the obtained results, exergy destruction of boiler, turbine, and condenser at full and half loads is the highest. Ahmadi and Toghraie [5] found that the boiler was the main source of wasting exergy at the Isfahan steam power plant.

Despite the extensive research on CEAM, this method does not incorporate the avoidable irreversibility and does not consider the precise interactions between components [6]. The Advanced Exergy Analysis Method (AEAM) determines how much of the exergy destruction achieved by the CEAM can be avoided and, also, determines how much of the exergy destruction in a component is caused by the inefficiency of other components [7]. This idea was firstly introduced by Morosuk and Tsatsaronis [8,9]. Nowadays, the AEAM is well implemented on various systems. Liao et al. [10] analyzed exhaust gas heat recovery in ORC-based combined systems and they, using AEAM, concluded that 25.65% of total exergy destruction was avoidable.

*. *Corresponding author.*
E-mail addresses: mahlaakhondi_mkh@gmail.com (M. Akhoundi); parisakazemiyani@yahoo.com (P. Kazemiani-Najafabadi); ehsanamech@gmail.com, a.amirirad@hsu.ac.ir (E. Amiri Rad)

doi: 10.24200/sci.2022.58742.5876

Ozcan et al. [11] simulated a solar PV-air source heat pump with a battery system. AEAM results revealed that the exergy destruction of all sections of the batteries was significant. The results of AEAM in an absorption-ejection refrigeration cycle by Chen et al. [12] indicate that generator and absorber have the first and second order of priority for optimization, because they have the most avoidable exergy destruction. Wang et al. [13] analyzed the exergetic performance of the dual-loop ORC used in engine waste heat recovery. The CEAM results showed that massive exergy destruction occurred in the high-temperature evaporator. In contrast, in AEAM, the priority for optimization is given to the low-temperature turbine. Wang et al. [14] evaluated the performance of a dual-loop ORC with a zeotropic mixture according to the AEAM. They found that the high-temperature turbine was the first component that should be repaired. Moreover, Liu et al. [15] assessed a transcritical CO_2 ejector refrigeration system integrated with a thermoelectric sub-cooler. The outcomes of AEAM revealed that the avoidable exergy destruction of the compressor was the highest, which differed from the outcomes of CEAM. Ebrahimi et al. [16] examined the Island underwater compressed air energy storage plant. The outcomes of CEAM indicated that the first optimization priority belonged to the turbine. However, following the application of the AEAM, one of the heat exchangers had the highest priority for optimization. Oyekale et al. [17] applied advanced exergoeconomic method to a hybrid solar-biomass ORC plant and found that 60% of irreversibility cost rates could be avoided. The advanced exergy, exergeconomic, and exergoenvironmental analyses on a heat pump aimed at space heating were studied by Voloshchuk et al. [18]. They reported that annual exergy destruction, annual cost of exergy of the product, and annual environmental impact were reduced upon improving system performance.

The Kalina cycle is one of the cycles used to generate electricity from low-temperature geothermal heat sources, which was first proposed by Alexander Kalina in 1984 [19]. Worldwide, only one plant based on KSC-34 principles was built in Husavik, Iceland, with an installed capacity of 2 MW [20]. Some studies have examined the Kalina cycle based on AEAM. Using AEAM, Fallah et al. [21] concluded that the improvement priority belonged to the condenser, turbine, and evaporator in the Kalina cycle, respectively. However, in the case of CEAM, improvement priority was given to the condenser, evaporator, and turbine, in order. AEAM results showed that the auxiliary heater and Parabolic-Trough Solar Collectors (PTSC) had the highest improvement priority in a Kalina cycle integrated with PTSC, as reported by Boyaghchi and Sabaghian [22].

Although the AEAM improves the outcomes of CEAM, it has some weaknesses that are as follows: a) The subjectivity associated with the definition of hybrid and ideal processes; and b) Requiring a significant number of simulations and calculations to achieve different parts of exergy destruction [23]. Therefore, due to the exhausting burden of calculations and complexity of the solution process in the AEAM, the probability of error occurring in calculations increases and, sometimes, the outputs of AEAM are not easily evaluated.

This paper presents a novel analysis method called the Extended Thermodynamic Analysis Method (ETAM) that overcomes the weaknesses of AEAM. ETAM is less complicated than the AEAM; in other words, there is no need to define ideal and hybrid processes. Therefore, the probability of error in calculations is reduced. However, the outcomes of ETAM and the AEAM are similar in determining the improvement priority of components. Generally, ETAM is composed of three sub-methods: extended energy analysis, extended entropy analysis, and extended exergy analysis. Therefore, the system is examined in terms of energy, entropy, and exergy and their results are confirmed by each other. In this study, a Kalina Cycle System-34 (KCS-34) is considered to produce power from low-temperature geothermal sources. KCS-34 is initially investigated using the CEAM and AEAM and then, by ETAM. Finally, the results of CEAM, AEAM, and ETAM are compared with each other to find the best strategy for enhancing the KCS-34 performance.

2. System configuration and assumptions

Kalina power cycles have different configurations based on the cycle applications. KCS-34 is one of the most used cycles for power generation from geothermal energy. The working fluid of all Kalina cycles is ammonia-water mixture with different boiling and condensation points at constant pressure [24]. Thus, the heat source (sink source) and the working fluid can have a better heat matching in the evaporator (condenser), which improves the performance of the Kalina cycle [25]. A schematic view of the KCS-34 is shown in Figure 1. The main components of a KCS-34 include a turbine, a generator, an evaporator, a separator, a Low-Temperature Recuperator (LTR), a High-Temperature Recuperator (HTR), a condenser, a pump, an expansion valve, and a mixer. In KCS-34, the ammonia-water mixture absorbs heat from the heat source in the evaporator (s8 $\rightarrow$ s9) and the hot two-phase flow enters a separator. Then, the rich ammonia vapor from poor ammonia liquid (s9 $\rightarrow$ s10, s9 $\rightarrow$ s1) is separated. The rich ammonia flow goes to the turbine for power generation (s1 $\rightarrow$ s2) and, then, enters the mixer. The poor ammonia liquid, after passing the HTR and expansion valve, is mixed with turbine outlet flow (s2, s12 $\rightarrow$ s3). Next, the ammonia-water mixture flows into LTR and

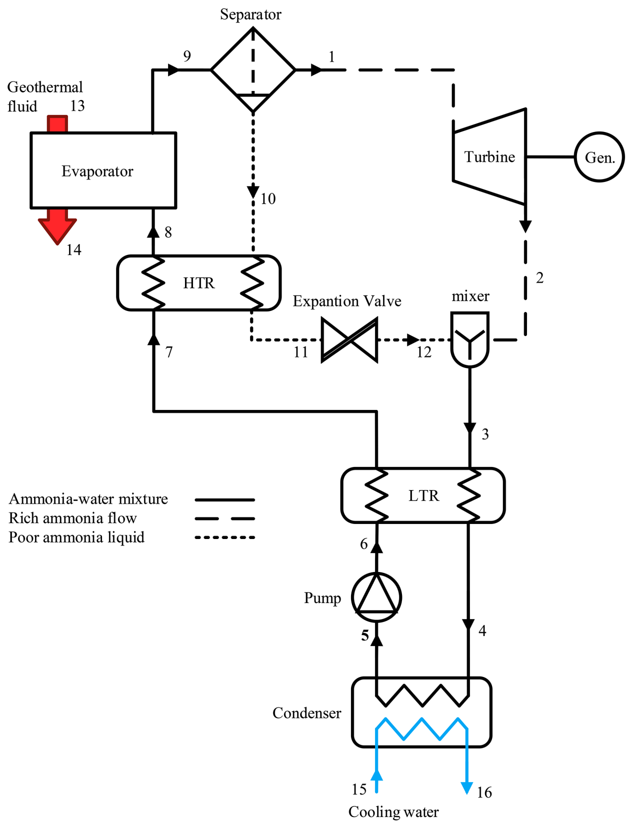

Figure 1. Schematic diagram of the KCS-34.

Table 1. Inlet parameters for KSC-34 simulation [26].

Parameter	Unit	Value
x	kg NH_3/kg solution	0.82
$\dot{m}_{gf}$	kg/s	89
$T_{gf,in}$	°C	122
$P_{gf,in}$	bar	2.5
$P_{gf,out}$	bar	2.5
T_{15}	°C	5
T_{16}	°C	18
P_{15}	bar	1.2
P_{16}	bar	1.2

eventually, the condensed liquid at the condenser outlet is pumped to the maximum pressure of the cycle. Then, the pumped mixture is pre-heated by passing through LTR and HTR and is sent into the evaporator (s6 → s7 → s8), and all processes start over [20].

The inlet parameters used for simulating the KSC-34 performance are listed in Table 1 [26].

To simulate the system, general assumptions are considered given below [27–29]:

- The system works in steady-state conditions;
- The variations in potential and kinetic energies are neglected;
- Specified isentropic efficiencies are considered for pump, turbine; and generator;
- The vapor and liquid flows at the separator outlet are considered saturated vapor and saturated liquid, respectively;
- The condenser outlet flow is assumed to be a saturated liquid.

3. Thermodynamic modeling

3.1. Energy analysis and CEAM

The equations of mass, energy and exergy for each control volume are expressed as follows:

$$\sum_{in} \dot{m} = \sum_{out} \dot{m}, \tag{1}$$

$$\dot{Q} - \dot{W} = \sum_{out} \dot{m}h - \sum_{in} \dot{m}h, \tag{2}$$

$$\dot{E}_Q - \dot{W} = \sum_{out} \dot{m}\psi - \sum_{in} \dot{m}\psi + \dot{E}_d, \tag{3}$$

where $\sum_{in} \dot{m}h$ and $\sum_{out} \dot{m}h$ indicate the energy transfer by mass flowing into or out of the control volume, respectively, $\sum_{in} \dot{m}\psi$ is the input flow exergy, and $\sum_{out} \dot{m}\psi$ is the output flow exergy. $\dot{E}_Q$ can be written as follows:

$$\dot{E}_Q = \sum_j (1 - T_0/T_j)\dot{Q}_j, \tag{4}$$

where $\dot{Q}_j$ is the heat transferred out of the system boundaries, T_j is instantaneous temperature, and T_0 is ambient temperature.

The flow exergy ($\dot{\Psi}$) can be divided into chemical exergy ($\dot{\Psi}^{CH}$), physical exergy ($\dot{\Psi}^{PH}$), potential exergy ($\dot{\Psi}^{PT}$), and kinetic exergy ($\dot{\Psi}^{KN}$). As assumed earlier, the variations in potential and kinetic energy are considered negligible and therefore, the exergy of flow j can be written as the sum of chemical and physical exergy [30]:

$$\dot{\Psi}_j = \dot{\Psi}_j^{CH} + \dot{\Psi}_j^{PH}. \tag{5}$$

The physical exergy of flow j can be computed via the following equation:

$$\dot{\Psi}_j^{PH} = \dot{m}\dot{\psi}_j^{PH} = \dot{m}\left[(h_j - h_0) - T_0\left(s_j - s_0\right)\right]. \tag{6}$$

Since the concentration of ammonia in Kalina cycle changes, chemical exergy variations should be considered. The chemical exergy of flow j can be obtained using following equation [31]:

$$\dot{\Psi}_j^{CH} = \dot{m}\psi_j^{CH} = \dot{m}\left[\left(\frac{\bar{\psi}_{NH_3}^{0,CH}}{M_{NH_3}}\right)x_j + \left(\frac{\bar{\psi}_{H_2O}^{0,CH}}{M_{H_2O}}\right)(x_j - 1)\right]. \tag{7}$$

In the above equation, $\bar{\psi}_{H_2O}^{0,CH}$ and $\bar{\psi}_{NH_3}^{0,CH}$ are the standard molar specific chemical exergy of water an-dammonia, and M_{H_2O} and M_{NH_3} are the molecular weights of water and ammonia, respectively [32].

The exergy balance for each system component (k) is represented as follows:

$$\dot{E}_{P,k} = \dot{E}_{F,k} - \dot{E}_{d,k}, \tag{8}$$

where $\dot{E}_{P,k}$, $\dot{E}_{F,k}$, and $\dot{E}_{d,k}$ are the product exergy, fuel exergy, and exergy destruction for the kth component, respectively [33]. The exergy balance for the whole system is stated as [34]:

$$\dot{E}_{P,tot} = \dot{E}_{F,tot} - \dot{E}_{d,tot} - \dot{E}_L = \dot{E}_{F,tot} - \dot{E}_w, \tag{9}$$

where $\dot{E}_L$ is the exergy loss of the whole system and it is associated with the transfer of exergy through material and energy streams to the surroundings, $\dot{E}_{d,tot}$ is total exergy destruction and is associated with the irreversibility within the system boundaries, and $\dot{E}_w$ is the wasted exergy which is the sum of the exergy loss and total exergy destruction. Moreover, Eqs. (10)–(13) are used to obtain the parameters required for the evaluation of system performance:

$$\varepsilon_k = \frac{\dot{E}_{P,k}}{\dot{E}_{F,k}} = 1 - \frac{\dot{E}_{d,k}}{\dot{E}_{F,k}}, \tag{10}$$

$$\eta_{exergy} = \frac{\dot{E}_{P,tot}}{\dot{E}_{F,tot}} = \frac{\dot{W}_{net}}{\dot{E}_{in}}, \tag{11}$$

$$y_k = \frac{\dot{E}_{d,k}}{\dot{E}_{F,k}} \times 100, \tag{12}$$

$$y_k^* = \frac{\dot{E}_{d,k}}{\dot{E}_{d,tot}} \times 100. \tag{13}$$

In the above equations, ε_k, η_{exergy}, y_k, and y_k^* are exergy efficiency of the kth component, total exergy efficiency, exergy destruction ratio, and relative exergy destruction, respectively. In addition, in Eq. (11), the total product exergy is the net output work of system and the total fuel exergy is input exergy to evaporator through heat transfer of geothermal working fluid. Table 2 lists the fuel and product exergies for the KCS-34 components.

3.2. AEAM

AEAM examines the interdependence between exergy destructions of components and the actual amount of component improvement priority [23]. In this method, the exergy destruction, which is an important parameter for analysis of the energy systems, can be divided into exogenous/endogenous and unavoidable/avoidable sections.

Table 2. Definition of fuel exergy and product exergy for KCS-34 components.

Component	$\dot{E}_{F,k}$	$\dot{E}_{P,k}$
Turbine	$\dot{\Psi}_1 - \dot{\Psi}_2$	$\dot{W}_{Turb}$
Pump	$\dot{W}_{Pump}$	$\dot{\Psi}_6 - \dot{\Psi}_5$
LTR	$\dot{\Psi}_3 - \dot{\Psi}_4$	$\dot{\Psi}_7 - \dot{\Psi}_6$
HTR	$\dot{\Psi}_{10} - \dot{\Psi}_{11}$	$\dot{\Psi}_8 - \dot{\Psi}_7$
Evaporator	$\dot{\Psi}_{13} - \dot{\Psi}_{14}$	$\dot{\Psi}_9 - \dot{\Psi}_8$
Condenser	$\dot{\Psi}_4 - \dot{\Psi}_5$	$\dot{\Psi}_{16} - \dot{\Psi}_{15}$
Separator	$\dot{\Psi}_9$	$\dot{\Psi}_1 + \dot{\Psi}_{10}$
Mixer	$\dot{\Psi}_2 - \dot{\Psi}_{12}$	$\dot{\Psi}_3$
Expansion valve	$\dot{\Psi}_{11} - \dot{\Psi}_{12}$	$\dot{m}_{11}(h_{11} - h_{12})$

The endogenous exergy destruction for a component ($\dot{E}_{d,k}^{EN}$) can be achieved when it works in real conditions, while other components work in ideal conditions. The exogenous exergy destruction ($\dot{E}_{d,k}^{EX}$) can be obtained by subtracting the endogenous exergy destruction from the exergy destruction.

$$\dot{E}_{d,k} = \dot{E}_{d,k}^{EN} - \dot{E}_{d,k}^{EX}. \tag{14}$$

The endogenous exergy destruction rate for the kth component is written as follows [35]:

$$\dot{E}_{d,k}^{EN} = \dot{E}_{P,k}\left(\frac{\dot{E}_{d,k}}{\dot{E}_{P,k}}\right)^{EN}, \tag{15}$$

where $\left(\dot{E}_{d,k}/\dot{E}_{P,k}\right)^{EN}$ is defined as exergy destruction to product exergy for the kth component in the hybrid cycle.

Different methods are currently available to calculate $\dot{E}_{d,k}^{EN}$. In this research, the thermodynamic cycle method is used to obtain $\dot{E}_{d,k}^{EN}$ and the accuracy of this method was demonstrated by Kelly et al. [34]. This method is the most suitable method for systems to operate based on a thermodynamic cycle [36].

The unavoidable exergy destruction ($\dot{E}_{d,k}^{UN}$) is a section of the component exergy destruction which cannot be eliminated due to technical limitations like accessibility, material cost, and production methods. Furthermore, the avoidable exergy destruction ($\dot{E}_{d,k}^{AV}$) can be achieved by subtracting the unavoidable exergy destruction from exergy destruction.

$$\dot{E}_{d,k} = \dot{E}_{d,k}^{UN} - \dot{E}_{d,k}^{AV}. \tag{16}$$

In order to account for the unavoidable exergy destruction of a component, the exergy efficiency of that component should be maximized. Under unavoidable conditions, the irreversibility is minimized and only the unavoidable irreversibility remains.

When a system is operating in unavoidable conditions, the unavoidable exergy destruction can be expressed as [30]:

$$\dot{E}_{d,k}^{UN} = \dot{E}_{P,k}\left(\frac{\dot{E}_{d,k}}{\dot{E}_{P,k}}\right)^{UN}, \tag{17}$$

where $(\dot{E}_{d,k}/\dot{E}_{P,k})^{UN}$ is the ratio of exergy destruction to product exergy for the kth component in unavoidable conditions.

By combining the endogenous, exogenous, avoidable and unavoidable exergy destructions for the kth component, it can be written that the sum of four exergy destruction sections is equal to conventional exergy destruction.

$$\dot{E}_{d,k} = \dot{E}_{d,k}^{EN,AV} + \dot{E}_{d,k}^{EN,UN} + \dot{E}_{d,k}^{EX,AV} + \dot{E}_{d,k}^{EX,UN}, \tag{18}$$

where $\dot{E}_{d,k}^{EN,AV}$ is avoidable endogenous exergy destruction, which is reduced upon improving the performance of the kth component and $\dot{E}_{d,k}^{EN,UN}$ is unavoidable endogenous exergy destruction, which cannot be reduced due to technological limitations of the kth component. $\dot{E}_{d,k}^{EX,AV}$ is avoidable exogenous exergy destruction, which can be reduced by improving the performance of other components, and $\dot{E}_{d,k}^{EX,UN}$ is unavoidable exogenous exergy destruction, which cannot be reduced due to technical limitations of the other components [37]. Different sections of $\dot{E}_{d,k}$ can be achieved via Eqs. (19)–(22):

$$\dot{E}_{d,k}^{EN,UN} = \dot{E}_{P,k}^{EN}\left(\frac{\dot{E}_{d,k}}{\dot{E}_{P,k}}\right)^{UN}, \tag{19}$$

$$\dot{E}_{d,k}^{EX,UN} = \dot{E}_{d,k}^{UN} - \dot{E}_{d,k}^{EN,UN}, \tag{20}$$

$$\dot{E}_{d,k}^{EN,AV} = \dot{E}_{d,k}^{EN} - \dot{E}_{d,k}^{EN,UN}, \tag{21}$$

$$\dot{E}_{d,k}^{EX,AV} = \dot{E}_{d,k}^{EX} - \dot{E}_{d,k}^{EX,UN}, \tag{22}$$

where $\dot{E}_{d,k}^{EN}$ is the endogenous product exergy for the kth component.

Ideal, real, hybrid, and unavoidable cycles are simulated to find different sections of the exergy destruction. In the ideal cycle, all processes are assumed reversible, while they are irreversible in the real cycle. In a hybrid cycle, the kth component operates in real conditions and other components operate in ideal conditions to calculate $\dot{E}_{d,k}^{EN}$. The number of hybrid conditions is equal to the number of components [37]. $\dot{E}_{d,k}^{UN}$ can be obtained using unavoidable cycle in which all components operate under unavoidable conditions. In unavoidable conditions, the improvement priority for system components is maximized despite technical limitations.

The improvement potential of each component can be obtained by dividing the avoidable exergy destruction of the component by its conventional exergy destruction [38].

$$IP_k = \frac{\dot{E}_{d,k}^{AV}}{\dot{E}_{d,k}}. \tag{23}$$

The assumptions required to analyze KCS-34 in the real, ideal, and unavoidable conditions are listed in Table 3. In this table, $\Delta T_{\min}$ is minimum temperature difference, ΔT_{pp} pinch point temperature difference, and ΔP is the pressure drop in the heat exchangers.

Table 3. Assumptions for the KCS-34 simulation under real, ideal, and unavoidable conditions.

Component	Parameter	Real/Ref.	Ideal	Unavoidable/Ref.
Condenser	$\Delta T_{\min}$	3 [26]	0	0.5 [40,41]
	$\Delta P_{4,5}$	17.33% [26]	0	1%
LTR	$\Delta T_{\min}$	5 [26]	0	0.5 [42]
	$\Delta P_{3,4}$	15.2% [26]	0	1% [21]
	$\Delta P_{6,7}$	2.8% [26]	0	1% [21]
HTR	$\Delta T_{\min}$	5 [26]	0	0.5 [42]
	$\Delta P_{7,8}$	2.9% [26]	0	1% [21]
	$\Delta P_{10,11}$	3.1% [26]	0	1% [21]
Evaporator	$\Delta T_{\min}$	6 [26]	0	0.5 [40,41]
	$\Delta P_{8,9}$	3% [26]	0	1% [21]
	ΔT_{pp}	5	0	3 [43]
Turbine	$\eta_{is,Turb}$	0.87 [26]	1	0.95 [44]
Pump	$\eta_{is,Pump}$	0.85 [39]	1	0.95 [43]
Expansion valve		Isenthalpic [40]	$\eta_{is,EXV} = 1$	Isenthalpic [40]
Generator	η_{Gene}	0.96 [26]	1	0.98 [21]

Also, for analysis of the ideal Kalina cycle, an isentropic expander is provided instead of expansion valve because the throttling process is irreversible.

It is noteworthy that the amount of net output power in the ideal and hybrid conditions ($\dot{W}_{net,ideal}$,$\dot{W}_{net,hybrid}$) is considered constant and equal to the net output power in real conditions ($\dot{W}_{net,real}$).

3.3. ETAM

As discussed, KCS-34 is investigated using a novel analysis method named ETAM in this study. ETAM is composed of 3 parts and each part can evaluate the system performance individually. These 3 parts include extended energy analysis, extended entropy analysis, and extended exergy analysis.

For each of the extended analyses, the Kalina cycle is simulated in both the real operating conditions and the reference operating conditions. Under the real conditions, both unavoidable and avoidable irreversibilities are considered for all of the system components (real cycle). In the reference conditions, the avoidable irreversibilities of a system component (e.g., kth component) are avoided, while the unavoidable irreversibilities of the component remain and other components operate under their real conditions (reference conditions for the kth component). In other words, in reference conditions, the kth component operates in unavoidable conditions, while the rest of components operate in real conditions. This process will be performed for each component in the system. Therefore, it can be said that the number of simulated cycles under the reference conditions (reference cycles) is equal to the number of the system components.

In extended energy analysis, by using energy balance equation (Eq. (2)), the following equation can be obtained:

$$\dot{W}_{net,ref_k} = \dot{W}_{Gene,ref_k} - \dot{W}_{Pump,ref_k}, \tag{24}$$

where $\dot{W}_{net,ref_k}$, $\dot{W}_{Gene,ref_k}$, and $\dot{W}_{Pump,ref_k}$ are net output power, generator power generation, and pump power consumption under the reference conditions for the kth component, respectively. It is clear that the improvement priority is given to the component that creates the most net output power under the reference conditions. The entropy balance equation is used for extended entropy analysis over a control volume which is written as follows [45]:

$$\sum \frac{\dot{Q}_j}{T_j} = \sum_{out} \dot{m}s - \sum_{in} \dot{m}s - \dot{S}_{gen}, \tag{25}$$

where $\sum \dot{Q}_j/T_j$ is the sum of the entropy transfer rates due to heat transfer, $\sum_{out} \dot{m}s$ and $\sum_{in} \dot{m}s$ are entropy transfer by mass flowing into or out of the control volume, respectively, and $\dot{S}_{gen}$ is the entropy generation in control volume. In extended entropy analysis, the total entropy generation is calculated under the reference conditions ($\dot{S}_{gen,tot,ref}$). The improvement priority is given to the component that leads to minimum total entropy generation in reference conditions.

In extended exergy analysis, the wasted exergy is calculated using exergy balance equation for the overall system (Eq. (9)) under the reference conditions ($\dot{E}_{w,ref}$). Then, the improvement priority is given to the component that leads to minimum wasted exergy under the reference conditions.

The energy and entropy balances for the KSC-34 components are summarized in Table 4. In this table, η_{is} is isentropic efficiency and x is the concentration of ammonia. Furthermore, subscripts ra, pa, gf, and cw denote rich ammonia flow, poor ammonia flow, geofluid, and cooling water, respectively.

Table 4. Thermodynamic equations for the KSC-34 components.

Component	Energy balance equations	Entropy balance equations
Turbine	$\dot{W}_{Turb} = \dot{m}_{ra}(h_1 - h_2)$	$\dot{S}_{gen,Turb} = \dot{m}_{ra}(s_2 - s_1)$
	$\eta_{is,Turb} = (h_1 - h_2)/(h_1 - h_{is,2})$	
Pump	$\dot{W}_{Pump} = \dot{m}(h_6 - h_5)$	$\dot{S}_{gen,Pump} = \dot{m}(s_6 - s_5)$
	$\eta_{is,Pump} = (h_{is,6} - h_5)/(h_6 - h_5)$	
LTR	$h_7 - h_6 = h_3 - h_4$	$\dot{S}_{gen,LTR} = \dot{m}(s_4 + s_7 - s_3 - s_6)$
HTR	$\dot{m}(h_8 - h_7) = \dot{m}_{pa}(h_{10} - h_{11})$	$\dot{S}_{gen,HTR} = \dot{m}(s_8 - s_7) + \dot{m}_{pa}(s_{11} - s_{10})$
Evaporator	$\dot{m}(h_9 - h_8) = \dot{m}_{gf}(h_{13} - h_{14})$	$\dot{S}_{gen,Evap} = \dot{m}(s_9 - s_8) + \dot{m}_{gf}(s_{14} - s_{13})$
Condenser	$\dot{m}_{cw}(h_{16} - h_{15}) = \dot{m}(h_4 - h_5)$	$\dot{S}_{gen,Cond} = \dot{m}(s_5 - s_4) + \dot{m}_{cw}(s_{16} - s_{15})$
Separator	$\dot{m}h_9 = \dot{m}_{ra}h_1 + \dot{m}_{pa}h_{10}$	$\dot{S}_{gen,Sep} = \dot{m}_{pa}s_{10} + \dot{m}_{ra}s_1 - \dot{m}s_9$
	$\dot{m}x = \dot{m}_{ra}x_{ra} + \dot{m}_{pa}x_{pa}$	
Mixer	$\dot{m}_{ra}h_2 + \dot{m}_{pa}h_{12} = \dot{m}h_3$	$\dot{S}_{gen,Mix} = \dot{m}s_3 - \dot{m}_{ra}s_2 - \dot{m}_{pa}s_{12}$
Expansion valve	$h_{11} = h_{12}$	$\dot{S}_{gen,EXV} = \dot{m}(s_{12} - s_{11})$

Table 5. Details of the model validation using the data reported by Fallah et al. [21].

	Enthalpy (kJ/kg)			Mass flow rate (kg/s)			Ammonia concentration ($kg\ NH_3/kg$ solution)		
Stream	**Ref.**	**Pres. value**	**Error (%)**	**Ref.**	**Pres. value**	**Error (%)**	**Ref.**	**Pres. value**	**Error (%)**
1	1411	1411	0	21.39	21.39	0	0.99	0.9899	0.01
2	1326	1326	0	21.39	21.39	0	0.99	0.9899	0.01
3	847.4	847.3	0.01	33.98	33.98	0	0.84	0.84	0
4	797.4	797.4	0	33.98	33.98	0	0.84	0.84	0
5	59.7	59.7	0	33.98	33.98	0	0.84	0.84	0
6	62.46	62.44	0.03	33.98	33.98	0	0.84	0.84	0
7	112.4	112.3	0.09	33.98	33.98	0	0.84	0.84	0
8	169.2	169.2	0	33.98	33.98	0	0.84	0.84	0
9	957.8	957.8	0	33.98	33.98	0	0.84	0.84	0
10	187	187	0	12.58	12.59	0.08	0.5852	0.5852	0
11	33.51	33.47	0.12	12.58	12.59	0.08	0.5852	0.5852	0
12	33.51	33.47	0.12	12.58	12.59	0.08	0.5852	0.5852	0

	Net output power (kW)	
Ref.	Present study	Error (%)
1672	1672	0

$T_9 = 90°C$, $P_9 = 25$ bar, $x_9 = 0.84$, Geofluid mass flow rate = 200 kg/s, Geofluid input temperature = 100°C

4. Results and discussion

4.1. Validation of the model

The data reported by Fallah et al. [21] are used to validate the outcome of the model proposed in this study. Fallah et al. [21] implemented CEAM and AEAM on a Kalina cycle applied to the enhanced geothermal power plant. Table 5 compares the thermodynamic data and mass flow rate results, and Figure 2 compares the different sections of exergy destruction for Kalina cycle components. As presented in Table 4 and Figure 2, the comparison of the outcomes shows that the data obtained in the current study and the data reported by Fallah et al. [21] are in agreement. Following the validation of the presented model, the Kalina cycle is evaluated using the proposed novel method called ETAM.

4.2. Energy analysis and CEAM

Table 6 indicates the thermodynamic properties for different state points of KCS-34 in real, ideal, and unavoidable conditions, respectively. In addition, the values obtained for turbine power, pump power, net output power, energy efficiency, and total exergy efficiency are given in Table 7. Given that the $\dot{W}_{net}$ of the ideal cycle is assumed equal to $\dot{W}_{net}$ of the real cycle, the mass flow rate of the ideal cycle will be less than that of the real cycle. Thus, although the difference between input and output specific enthalpies of the turbine in the ideal cycle is larger than that in the real cycle, the turbine power in the ideal cycle is lower. It is the same for the unavoidable cycle.

The outcomes of CEAM on KCS-34 in real, ideal, and unavoidable conditions are given in Tables 8–10, respectively. In CEAM, the improvement priority is given to components with greater exergy destruction. According to Table 8, the maximum exergy destruction in real conditions belongs to the condenser, followed by the evaporator, turbine, LTR, and HTR, while the pump has the lowest exergy destruction.

4.3. AEAM

The process of calculating the exergy destructions for the kth component and corresponding equations are shown in the flowchart of Figure 3.

The outcomes of AEAM of the KCS-34 are listed in Table 11. By dividing the exergy destruction into exogenous and endogenous parts (second and third columns of Table 11), the following outcomes are obtained:

- In the investigated components, $\dot{E}_{d,k}^{EN}$ is greater than

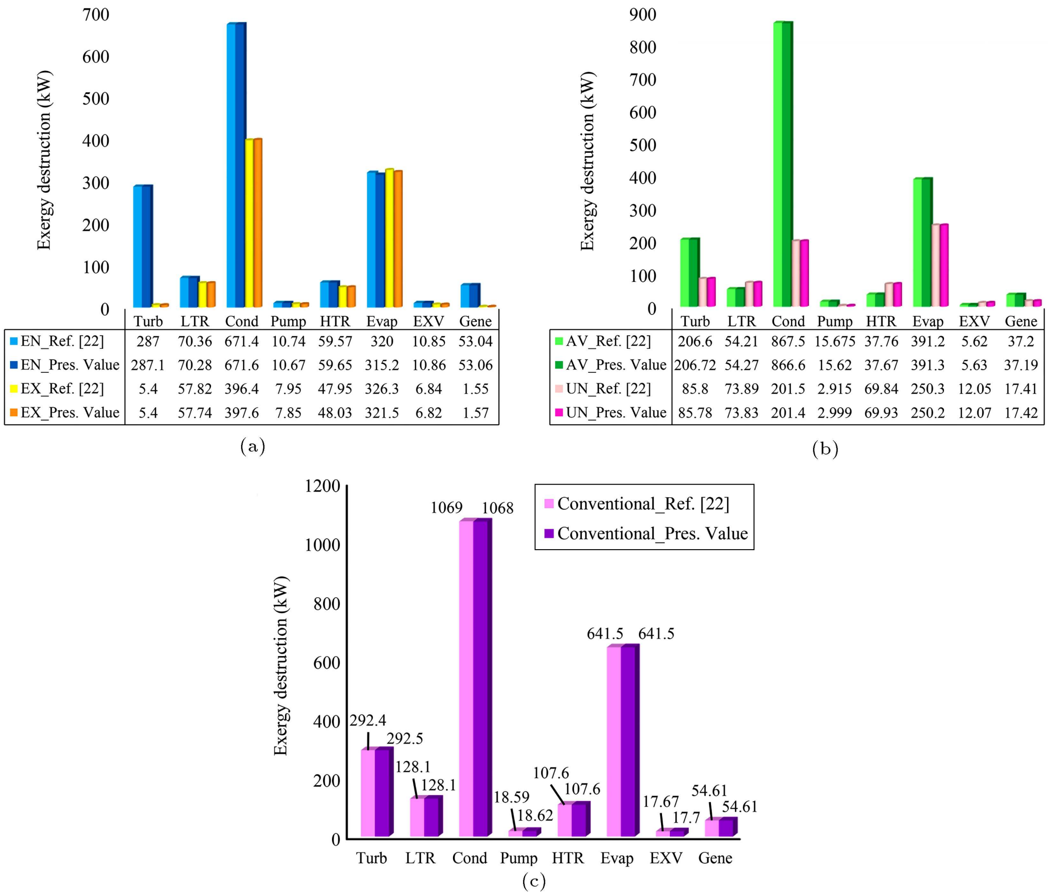

Figure 2. Comparison of the exergy destruction of: (a) endogenous and exogenous, (b) avoidable and unavoidable, and (c) conventional in the present study with those reported in Ref. [21].

Table 6. Thermodynamic parameters of KCS-34 in real, ideal, and unavoidable conditions.

State	Fluid	Real			Ideal			Unavoidable		
		h (kj/kg)	$\dot{m}$ (kg/s)	$\dot{\Psi}$ (kW)	h (kj/kg)	$\dot{m}$ (kg/s)	$\dot{\Psi}$ (kW)	h (kj/kg)	$\dot{m}$ (kg/s)	$\dot{\Psi}$ (kW)
1	NH_3H_2O	1481	11.32	222934	1494	7.702	141338	1497	7.924	155276
2	NH_3H_2O	1276	11.32	220310	1192	7.702	139166	1217	7.924	152954
3	NH_3H_2O	841.2	16.89	276813	776.4	10.58	172965	806.6	11.54	188764
4	NH_3H_2O	698.2	16.89	276361	667.4	10.58	172875	686.6	11.54	188637
5	NH_3H_2O	–90.42	16.89	275621	–104.4	10.58	172632	–102.1	11.54	188334
6	NH_3H_2O	–85.38	16.89	275694	–100.1	10.58	172678	–97.53	11.54	188384
7	NH_3H_2O	57.59	16.89	275860	8.964	10.58	172734	22.44	11.54	188458
8	NH_3H_2O	169.5	16.89	276136	148.5	10.58	172921	153.8	11.54	188659
9	NH_3H_2O	1091	16.89	279868	1122	10.58	175462	1130	11.54	191421
10	NH_3H_2O	300	5.572	56934.5	329.6	3.375	34124	326.1	3.62	36144
11	NH_3H_2O	–39.38	5.572	56523.5	–107.8	3.375	33821	–93	3.62	35827
12	NH_3H_2O	–39.38	5.572	56508.5	–111.6	3.375	33808	–93	3.62	35816
13	H_2O	512.3	89	7514	512.3	53.6	4525	512.3	62.5	5277
14	H_2O	337.3	89	3437	320	53.6	1871	332.1	62.5	2342
15	H_2O	21.14	244.7	7.412	21.14	150	4.544	21.14	167.2	5.065
16	H_2O	75.58	244.7	402.8	75.58	150	246.9	75.58	167.2	275.3

Table 7. The results of energy analysis.

Parameters	Real	Ideal	Unavoidable
$\dot{W}_{Turb}$ (kW)	2317	2172	2214
$\dot{W}_{Pump}$ (kW)	85.2	45.87	52.58
$\dot{W}_{net}$ (kW)	2139	2139	2139
η_{energy} (%)	0.1269	0.2075	0.1899
η_{exergy} (%)	0.4849	0.8058	0.7289

$\dot{E}_{d,k}^{EX}$. It means that the highest exergy destruction of each component is caused by the internal irreversibility of the component itself. Thus, the interdependence between the components is not strong;

- $\dot{E}_{d,k}^{EX}$ in condenser is 119.9 kW which is 31.98% of the total exogenous exergy destruction ($\dot{E}_{d,tot}^{EX}$), followed by LTR (115.7 kW) and evaporator (104.5 kW). Therefore, the improvement of the remaining components can significantly reduce the exergy destruction of these three components.

To assess the real potential for component improvement, the exergy destruction is also divided into avoidable and unavoidable parts (fourth and fifth columns of Table 11) and the following conclusions are found:

- The value of $\dot{E}_{d,k}^{AV}$ in condenser and LTR is much greater than $\dot{E}_{d,k}^{UN}$. This shows that these two components can be significantly modified using technological enhancement;
- The highest $\dot{E}_{d,k}^{AV}$ belongs to condenser, followed

Table 8. CEAM results for KCS-34 under real conditions.

Component	$\dot{E}_{F,k}$ (kW)	$\dot{E}_{P,k}$ (kW)	$\dot{E}_{d,k}$ (kW)	ε_k (%)	$y_k = \dot{E}_{d,k}/\dot{E}_{F,k}$ (%)	$y_k^* = \dot{E}_{d,k}/\dot{E}_{d,tot}$ (%)
Turbine	2624	2317	307	88.3	11.7	19.96
LTR	453.5	167	286.5	36.8	63.18	18.63
Condenser	740.8	395.7	345	53.4	46.58	22.43
Pump	85.2	72.67	12.53	85.3	14.71	0.815
HTR	410.7	276	134.7	67.2	32.79	8.755
Evaporator	4076	3731	344.6	91.54	8.455	22.41
Expansion valve	15	0	15	0	100	0.975
Generator	2317	2224	92.69	95.99	4	6.026
Overall system	4076	2139	1538.02	52.48	37.73	100

Table 9. CEAM results for KCS-34 under ideal conditions.

Component	$\dot{E}_{P,k}$ (kW)	$\dot{E}_{F,k}$ (kW)	$\dot{E}_{d,k}$ (kW)	ε_k (%)	$y_k = \dot{E}_{d,k}/\dot{E}_{F,k}$ (%)	$y_k^* = \dot{E}_{d,k}/\dot{E}_{d,tot}$ (%)
Turbine	2172	2172	0	100	0	0
LTR	89.98	55.66	34.32	61.86	38.14	13.04
Condenser	242.5	242.4	0.1505	99.94	0.062	0.572
Pump	45.87	45.87	0	100	0	0
HTR	303.3	187.9	115.4	61.96	38.04	43.8
Evaporator	2654	2541	113.5	95.72	4.276	43.13
Expansion valve	12.72	12.72	0	100	0	0
Generator	2172	2172	0	100	0	0
Overall system	2654	2139	263.2	80.58	9.916	100

Table 10. CEAM results for KCS-34 under unavoidable conditions.

Component	$\dot{E}_{F,k}$ (kW)	$\dot{E}_{P,k}$ (kW)	$\dot{E}_{d,k}$ (kW)	ε_k (%)	$y_k = \dot{E}_{d,k}/\dot{E}_{F,k}$ (%)	$y_k^* = \dot{E}_{d,k}/\dot{E}_{d,tot}$ (%)
Turbine	2322	2214	108.2	95.34	4.658	20.82
LTR	127.5	73.89	53.62	57.95	42.05	10.32
Condenser	302.5	270.2	32.25	89.34	10.66	6.208
Pump	52.58	49.98	2.601	95.05	4.948	0.5007
HTR	317.1	200.9	116.2	63.35	36.65	22.37
Evaporator	2935	2762	172.8	94.11	5.888	33.36
Expansion valve	11.72	0	11.72	0	100	2.256
Generator	2214	2192	22.14	99	1	4.261
Overall system	2935	2139	519.5	72.89	17.7	100

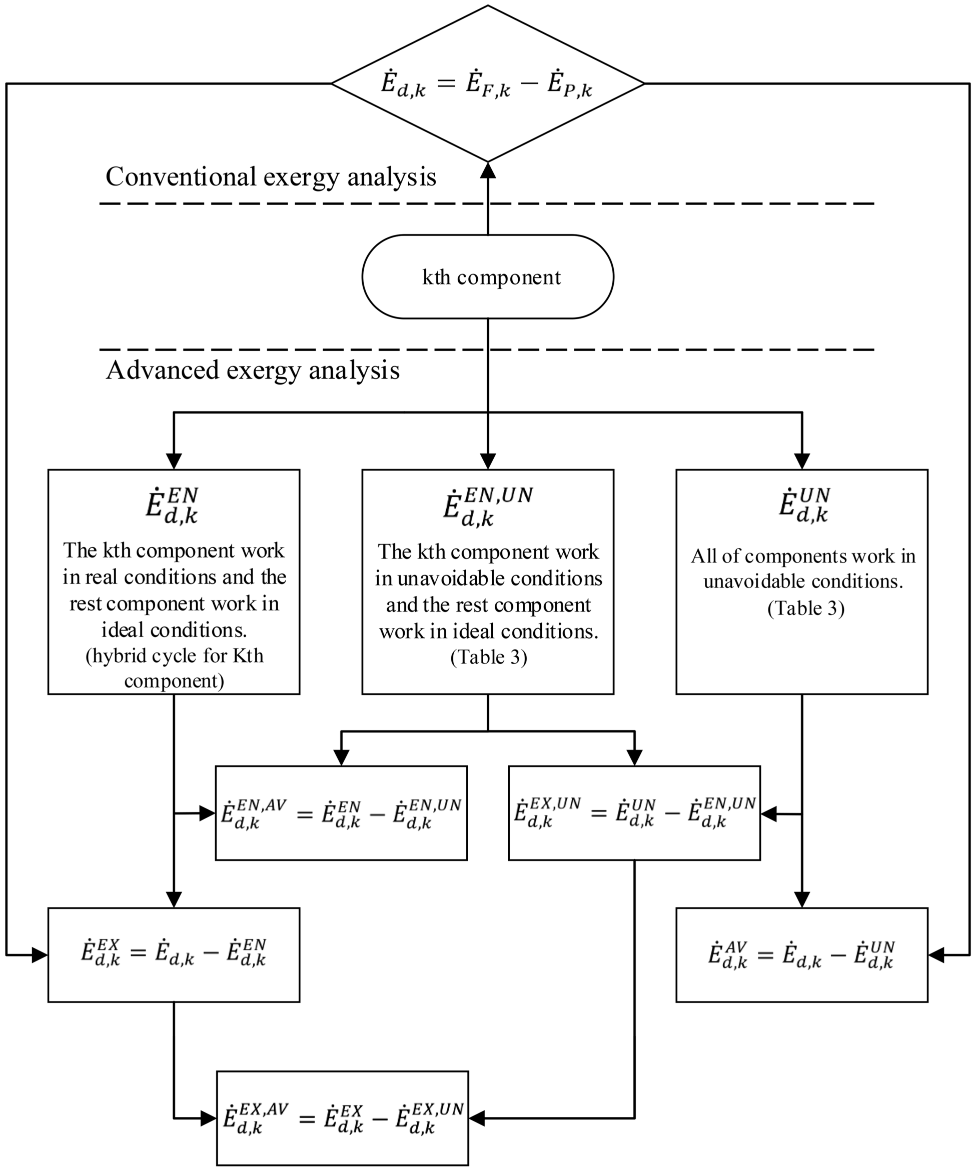

Figure 3. Flowchart of calculating the exergy destructions for the kth component (conventional and advanced).

Table 11. Results of AEAM.

Component	$\dot{E}_{d,k}$ (kW)	$\dot{E}_{d,k}^{EN}$ (kW)	$\dot{E}_{d,k}^{EX}$ (kW)	$\dot{E}_{d,k}^{AV}$ (kW)	$\dot{E}_{d,k}^{UN}$ (kW)	$\dot{E}_{d,k}^{EN,AV}$ (kW)	$\dot{E}_{d,k}^{EN,UN}$ (kW)	$\dot{E}_{d,k}^{EX,AV}$ (kW)	$\dot{E}_{d,k}^{EX,UN}$ (kW)	IP_k (%)
Turbine	307	302.6	4.4	198.8	108.2	195.5	107.1	3.3	1.1	64.76
LTR	286.5	170.8	115.7	232.88	53.62	126.19	44.61	106.69	9.01	81.28
Condenser	345	225.1	119.9	312.75	32.25	202.96	22.14	109.79	10.11	90.65
Pump	12.53	8.052	4.478	9.929	2.601	5.656	2.396	4.273	0.205	79.24
HTR	134.7	114.2	20.5	18.5	116.2	–0.1	114.3	18.6	1.9	13.73
Evaporator	344.6	240.1	104.5	171.8	172.8	80.4	159.7	91.4	13.1	49.85
Expansion valve	15	11.69	3.31	3.28	11.72	0	11.69	3.28	0.03	21.87
Generator	92.69	90.56	2.13	70.55	22.14	68.62	21.94	1.93	0.2	76.11
Overall system	1538.02	1163.10	374.92	1018.49	519.53	679.23	483.88	339.26	35.655	66.22

by LTR, turbine and evaporator, which account together for 89.96% (916.23 kW) of the total avoidable exergy destruction;

- In evaporator, HTR, and expansion valve, $\dot{E}_{d,k}^{UN}$ is greater than $\dot{E}_{d,k}^{AV}$. This implies that improvement of these components has no remarkable impact on improving the system efficiency;
- In the studied cycle, up to 1018.49 kW or 66.22% of total exergy destruction can be avoided and hence, the system has high potential for efficiency improvement.

Considering the combination of exogenous/ endogenous and unavoidable/avoidable exergy destruction, it can be divided into four sections (sixth to ninth columns of Table 11). As revealed, in most of the components, $\dot{E}_{d,k}^{AV}$ is greater than $\dot{E}_{d,k}^{UN}$ which means that the improvement of that component can reduce the exergy destruction in that component and other system components. Therefore, $\dot{E}_{d,k}^{EX,AV}$ and $\dot{E}_{d,k}^{EN,AV}$ should be considered. It is concluded that:

- The highest $\dot{E}_{d,k}^{EX,AV}$ belongs to the condenser, followed by LTR and evaporator. This shows that the efficiency improvement of other components has greater effect on reduction of exergy destruction in these three components;
- The highest $\dot{E}_{d,k}^{EN,AV}$ belongs to condenser, followed by turbine and LTR, which account together for 77.24% (524.65 kW) of total avoidable endogenous exergy destruction ($\dot{E}_{d,tot}^{EN,AV}$). Technical improvement of these components can significantly reduce the total exergy destruction and increase the system efficiency;
- Improvement of a component with higher $\dot{E}_{d,k}^{EN,AV}$ can have substantial effect on the reduction of system exergy destruction without any impact on exergy destruction of the other components. AEAM suggests that the first priority of improvement should be given to the condenser because it accounts for 29.88% of $\dot{E}_{d,tot}^{EN,AV}$, followed by turbine, LTR, evaporator, generator, and pump;
- IP parameter can be used to identify the improvement potential of each component [46]. According to the last column of Table 11, the condenser has the highest IP value; thus, after improving the system, 90.65% of condenser exergy destruction can be avoided, followed by LTR, pump, generator, and turbine. Also, the IP for the whole system is determined to be 66.22%, which shows that the system has significant potential for improvement. In some studies, IP parameter is used to prioritize components [36];
- The avoidable endogenous exergy destruction of HTR ($\dot{E}_{d,HTR}^{EN,AV}$) is negative. Because $\dot{E}_{d,HTR}^{EN,UN} \rangle \dot{E}_{d,HTR}^{EN}$, it can be inferred that $\dot{E}_{d,HTR}^{EN,AV} \langle 0$. The negative sign indicates that the increase in the HTR irreversibility leads to a decrease in $\dot{E}_{d,HTR}^{EN,AV}$. In fact, when HTR irreversibility is increased, both product and fuel exergies are increased such that their difference (i.e., HTR exergy destruction) is reduced [47].

4.4. ETAM

As discussed, the AEAM enhances the accuracy of exergy analysis. However, among its weaknesses are the large number of required simulations and complexity of the solving procedure. For this reason, in this research, a novel analysis called ETAM is proposed. This novel method is easier than AEAM, while the outcomes of both methods are similar for determining the improvement priority of components.

ETAM is used in this study to investigate the low-temperature geothermal source driven-KCS-34. In ETAM, KCS-34 is simulated under reference conditions. In reference conditions, a component works in unavoidable conditions and the rest of components work in real conditions. Thus, the number of reference conditions is equal to the number of system components.

The objective function is selected based on the type of the system (power generation, heat generation, and so on). In extended energy analysis, for KCS-34 as a power generation cycle, the net output power is taken into account as the objective function. The improvement priority is given to the component that leads to highest net output power under the reference conditions. In extended entropy analysis, the total entropy generation is considered as the objective function and the improvement priority is given to the component that leads to the lowest total entropy generation under the reference conditions in the whole cycle. Moreover, in the extended exergy analysis, the wasted exergy of the system is calculated as the objective function. Here, the improvement priority is given to the component that minimizes the wasted exergy under the reference conditions.

The results obtained from ETAM are presented in Table 12. This table lists the amount of net output power, total entropy generation, and wasted exergy under the reference and real conditions. Also, the improvement percentage of these parameters is shown in Figure 3. As seen in Figure 4, in the reference conditions for HTR (i.e., when HTR works under unavoidable conditions and the rest of the components work in real conditions), the improvement percentages of $\dot{W}_{net,ref_{HTR}}$, $\dot{S}_{gen,tot,ref_{HTR}}$, and $\dot{E}_{w,ref_{HTR}}$ are negative. It means that the net output power decreases by improving HTR, while the total entropy generation and wasted exergy increase. According to Eq. (9), after subjecting HTR to reference conditions, it is

Table 12. Results of extended thermodynamic analysis.

Component	$\dot{W}_{net,ref_k}$ (kW)	$\dot{S}_{gen,tot,ref_k}$ (kW/K)	$\dot{E}_{w,ref_k}$ (kW)
Turbine	2344	7.828	2503
LTR	2276	8.014	2580
Condenser	2428	7.594	2412
Pump	2148	8.506	2698
HTR	2117	8.563	2736
Evaporator	2241	8.213	2604
Expansion valve	2139	8.538	2706
Generator	2209	8.286	2637

$\dot{W}_{net,real} = 2139$ (kW), $\dot{S}_{gen,tot,real} = 8.538$ (kW/K), $\dot{E}_{w,real} = 2706$ (kW).

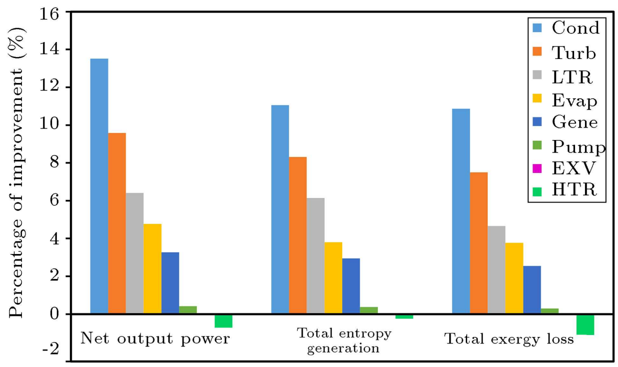

Figure 4. Improvement percentage of net output power, total entropy generation, and wasted exergy for different components under the reference conditions.

observed that $\dot{E}_{d,HTR}$ and, as a result, $\dot{E}_{d,tot}$ decrease, but $\dot{E}_L$ increases which leads to increase in wasted exergy. Regarding the net output power, the pressure ratio of the turbine increases with the improvement of HTR, while the mass flow rate of the system decreases. Moreover, the difference in the enthalpy of the turbine and the pump does not change much. Therefore, the powers of the turbine and pump are reduced and this, in turn, reduces the net output power. In addition, the reduction of the mass flow rate causes an increase in total entropy generation.

According to Figure 4, the priority of components for improvement using extended energy, entropy, and exergy analyses is similar. For instance, when condenser is under the reference conditions, the highest improvement percentages of 13.5%, 11.05%, and 10.86% are obtained for $\dot{W}_{net,ref_{Cond}}$, $\dot{S}_{gen,tot,ref_{Cond}}$, and $\dot{E}_{w,ref_{Cond}}$, respectively. Therefore, the condenser is considered as the first priority for improvement, while expansion valve and HTR are not included. Obviously, three parts of the extended analyses lead to the same improvement priority. Then, it is concluded that the calculations of the model are correctly performed.

4.5. Comparison of CEAM, AEAM, and ETAM

As mentioned earlier, in CEAM, the improvement priority is related to the component with the highest exergy destruction, while in AEAM, the priority belongs to the component with the highest $\dot{E}_d^{EN,AV}$. Moreover, in ETAM, the improvement priority is given to the component that leads to the highest improvement in $\dot{W}_{net,ref}$, $\dot{S}_{gen,tot,ref}$, and $\dot{E}_{w,ref}$ in its reference condition. Based on the results presented in Tables 8, 11, and 12, the improvement priority for KCS-34 components is shown in Figure 5 (The bigger the number, the lower priority for optimization) and the following findings are obtained:

- Using CEAM and AEAM, different improvement priorities are achieved for components. For example, in CEAM, the condenser and evaporator experience the highest irreversibility due to the two-phase transition processes. Therefore, the first and second improvement priorities are given to these two components. However, in AEAM, the evaporator has the fourth order of improvement priority, because a large section of the exergy destruction in the evaporator is unavoidable;
- The results obtained using 3 parts of ETAM (including extended energy, extended entropy, and extended exergy analyses) are confirmed by each other;
- Based on the comparison of the outcomes from AEAM and ETAM, it is found that the improvement priority of the system components is similar in both methods, while ETAM is clearly easier and also is a self-validated method.

5. Conclusions

This study presented a novel Extended Thermodynamic Analysis Method called ETAM for better evaluation of the thermodynamic cycles. This method intro-

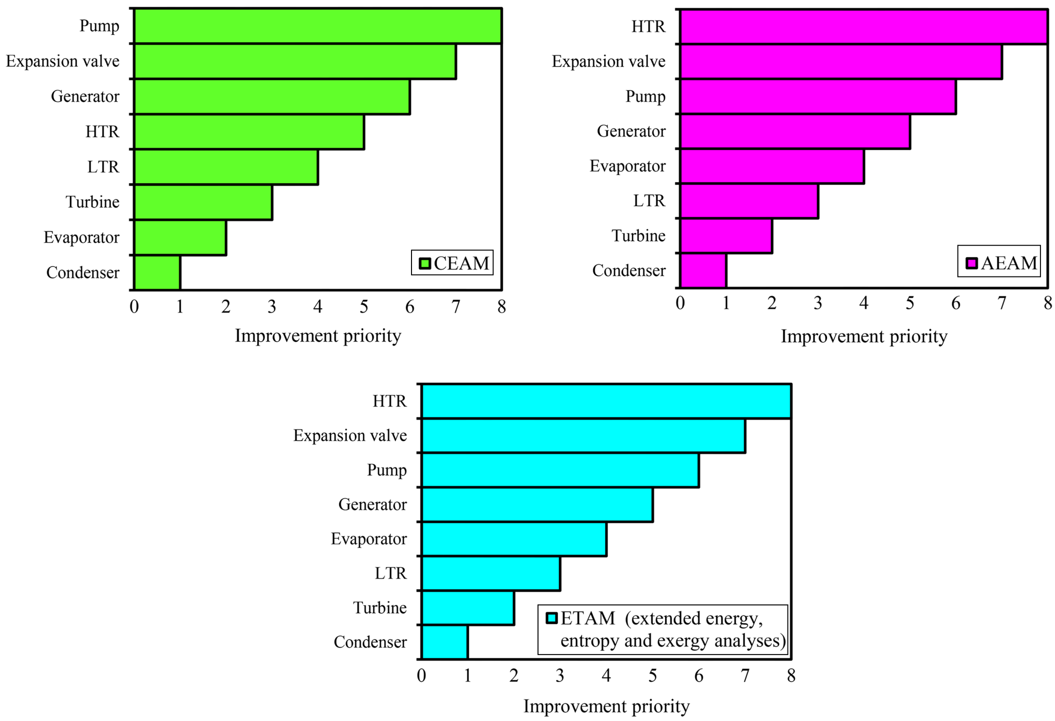

Figure 5. Improvement priority of components in KCS-34.

duced the best strategy for determining the improvement priority of components compared to Conventional Exergy Analysis Method (CEAM) and Advanced Exergy Analysis Method (AEAM). ETAM was found more accurate than the CEAM and less complex than the AEAM. It was composed of three different parts, including extended energy analysis, extended entropy analysis, and extended exergy analysis. Then, after total analysis, the results of different parts confirmed each other and, consequently, ETAM was considered a self-validated method.

To investigate ETAM, this method was used to evaluate a low-temperature geothermal Kalina cycle system-34 and the priority of components for improvement was determined and compared with the outputs of CEAM and AEAM. The main conclusions are as follows:

- In part I, in the case of extended energy analysis, the improvement priority of components is given to condenser, turbine, and Low-Temperature Recuperator (LTR), respectively. By subjecting these three components to reference conditions, the highest net output power with values of the 2428 kW, 2344 kW, and 2276 kW was achieved for the system, respectively;
- In Part II: According to the extended entropy analysis, by subjecting condenser, turbine, and LTR to reference conditions, the lowest total entropy generation with values of the 7.594 kW/K, 7.828 kW/K, and 8.014 kW/K was obtained for the system, respectively. Hence, the improvement priority was given to these components, again;
- Part III: Extended exergy analysis indicates that the lowest wasted exergy occurred in condenser, turbine, and LTR with values of the 2412 kW, 2503 kW, and 2580 kW under the reference conditions. Therefore, the first, second, and third priorities of improvement belonged to these three components, respectively;
- In case no validation is required, one of the three parts of ETAM would be sufficient to determine the improvement priority for components. However, in case evaluation and validation of results were required, two or three parts of ETAM could be performed. The results obtained using three parts of ETAM confirmed each other and, hence, ETAM validated itself automatically;
- According to the CEAM, the most exergy destruction belonged to the condenser, evaporator, and turbine, respectively. However, following the use of AEAM, the improvement priority of components was given to condenser, turbine, and LTR, respectively, due to higher avoidable endogenous exergy destruction. This difference in improvement priority occurs because the AEAM considers the interdependence between components and real potential for components improvement;
- Based on the comparison of the outcomes of ETAM and AEAM, it can be concluded that the improvement priority of the system components was similar in both methods. However, in advanced exergy

analysis, the complexity of the solution and the number of simulations required to obtain different sections of exergy destruction were much greater than ETAM.

Nomenclature

Symbols

$\dot{E}$	Exergy (kW)
h	Specific enthalpy (kJ/kg)
M	Molar
$\dot{m}$	Mass flow rate (kg/s)
P	Pressure (bar)
$\dot{Q}$	Heat transfer rate (kW)
Qu	Quality
s	Specific entropy (kJ/kg.K)
$\dot{S}$	Entropy (kW/K)
T	Temperature (K)
$\dot{W}$	Power (kW)
x	Ammonia concentration

Abbreviations

HTR	High Temperature Recuperator
LTR	Low Temperature Recuperator
s	State

Subscripts

$Cond$	Condenser
cw	Cooling water
d	Destruction
$Evap$	Evaporator
EXV	Expansion valve
F	Fuel
gen	Generation
$Gene$	Generator
gf	Geothermal fluid
in	Inlet
is	Isentropic
k	Component
L	Loss
min	Minimum
Mix	Mixer
out	Outlet
P	Product
pa	Poor ammonia flow
pp	Pinch point
Q	Heat transfer
ra	Rich ammonia flow
ref	Reference condition
Sep	Separator
tot	total
$Turb$	Turbine
$1, 2, ...$	Flow number
0	Reference state

Superscrips

AV	Avoidable
CH	Chemical
EN	Endogenous
EX	Exogenous
KN	Kinetic
PH	Physical
PN	Potential
UN	Unavoidable
0	Standard state

Greek symbols

η	Efficiency
ε	Exergy efficiency
ψ	Specific exergy flow (kJ/kg)
$\dot{\Psi}$	Exergy flow (kW)

References

1. Tsatsaronis, G. "Definitions and nomenclature in exergy analysis and exergoeconomics", *Energy*, **32**(4), pp. 249–253 (2007).
2. Hatami, S., Payehaneh, G., and Mehrpanahi, A. "Energy and exergy analysis of an indirect solar dryer based on a dynamic model", *J. Clean. Prod.*, **244**, 118809 (2019).
3. Ghorbani, B., Mehrpooya, M., and Ardehali, A. "Energy and exergy analysis of wind farm integrated with compressed air energy storage using multi-stage phase change material", *J. Clean. Prod.*, **259**, 120906 (2020).
4. Elhelw, M., Al Dahma, K.S., and Attia, A.E.H. "Utilizing exergy analysis in studying the performance of steam power plant at two different operation mode", *Appl. Therm. Eng.*, **150**, pp. 285–293 (2019).
5. Ahmadi, G.R. and Toghraie, D. "Energy and exergy analysis of Montazeri steam power lpant in Iran", *Renew. Sustain. Energy Rev.*, **56**, pp. 454–463 (2016).
6. Yan, C., Yang, A., Chien, I.-L., et al. "Advanced exergy analysis of organic Rankine Cycles for Fischer-Tropsch syngas production with parallel dry and steam methane reforming", *Energy Convers. Manag.*, **199**, 111963 (2019).
7. Yuan, B., Zhang, Y., Du, W., et al. "Assessment of energy saving potential of an industrial ethylene cracking furnace using advanced exergy analysis", *Appl. Energy*, **254**, 113583 (2019).

8. Morosuk, T. and Tsatsaronis, G. "A new approach to the exergy analysis of absorption refrigeration machines", *Energy*, **33**(6), pp. 890–907 (2008).
9. Morosuk, T. and Tsatsaronis, G. "Advanced exergy-based methods used to understand and improve energy-conversion systems", *Energy*, **169**, pp. 238–246 (2019).
10. Liao, G., Jiaqiang, E., Zhang, F., et al. "Advanced exergy analysis for Organic Rankine Cycle-based layout to recover waste heat of flue gas", *Appl. Energy*, **266**, 114891 (2020).
11. Ozcan, H.G., Varga, S., Gunerhan, H., et al. "Numerical and experimental work to assess dynamic advanced exergy performance of an on-grid solar photovoltaic-air source heat pump-battery system", *Energy Convers. Manag.*, **227**, 113605 (2021).
12. Chen, P., He, G., Gao, Y., et al. "Conventional and advanced exergy analysis of an air-cooled type of absorption-ejection refrigeration cycle with R290-mineral oil as the working pair", *Energy Convers. Manag.*, **210**, 112703 (2020).
13. Wang, Z., Hu, Y., and Xia, X. "Comparison of conventional and advanced exergy analysis for dual-loop organic rankine cycle used in engine waste heat recovery", *J. Therm. Sci.*, **30**(1), pp. 177–190 (2021).
14. Wang, Z., Xia, X., Pan, H., et al. "Fluid selection and advanced exergy analysis of dual-loop ORC using zeotropic mixture", *Appl. Therm. Eng.*, **185**, p. 116423 (2021).
15. Liu, X., Yu, K., Wan, X., et al. "Conventional and advanced exergy analyses of transcritical CO_2 ejector refrigeration system equipped with thermoelectric subcooler", *Energy Reports*, **7**, pp. 1765–1779 (2021).
16. Ebrahimi, M., Carriveau, R., Ting, D.S.K., et al. "Conventional and advanced exergy analysis of a grid connected underwater compressed air energy storage facility", *Appl. Energy*, **242**, pp. 1198–1208 (2019).
17. Oyekale, J., Petrollese, M., and Cau, G. "Modified auxiliary exergy costing in advanced exergoeconomic analysis applied to a hybrid solar-biomass organic Rankine cycle plant", *Appl. Energy*, **268**, 114888 (2020).
18. Voloshchuk, V., Gullo, P., and Sereda, V. "Advanced exergy-based performance enhancement of heat pump space heating system", *Energy*, **205**, 117953 (2020).
19. Kalina, A.I. "Combined-cycle system with novel bottoming cycle", *Journal of Engineering for Gas Turbines and Power*, **106**(4), pp. 737–742 (1984).
20. Arslan, O. "Exergoeconomic evaluation of electricity generation by the medium temperature geothermal resources, using a Kalina cycle: Simav case study", *Int. J. Therm. Sci.*, **49**(9), pp. 1866–1873 (2010).
21. Fallah, M., Mahmoudi, S.M.S., Yari, M., et al. "Advanced exergy analysis of the Kalina cycle applied for low temperature enhanced geothermal system", *Energy Convers. Manag.*, **108**, pp. 190–201 (2016).
22. Boyaghchi, F.A. and Sabaghian, M. "Advanced exergy and exergoeconomic analyses of Kalina cycle integrated with parabolic-trough solar collectors", *Sci. Iran.*, **23**(5), pp. 2247–2260 (2016).
23. Morosuk, T. and Tsatsaronis, G. "Strengths and limitations of advanced exergetic analyses", *Proceedings of the ASME 2013 International Mechanical Engineering Congress and Exposition IMECE2013*, pp. 1–11 (2013).
24. Kazemiani-Najafabadi, P. and Amiri, E. "Optimization of an improved power cycle for geothermal applications in Iran", *Energy*, **209**, 118381 (2020).
25. Wang, J., Yan, Z., Zhou, E., et al. "Parametric analysis and optimization of a Kalina cycle driven by solar energy", *Appl. Therm. Eng.*, **50**(1), pp. 408–415 (2013).
26. Ogriseck, S. "Integration of Kalina cycle in a combined heat and power plant, a case study", *Appl. Therm. Eng.*, **29**(14–15), pp. 2843–2848 (2009).
27. Kazemiani-Najafabadi, P., Amiri Rad, E., and Simonson, C.J. "Designing and thermodynamic optimization of a novel combined absorption cooling and power cycle based on a water-ammonia mixture", *Energy*, **253**, 124076 (2022).
28. Kazemiani-Najafabadi, P. and Amiri Rad, E. "Multi-objective optimization of a novel offshore CHP plant based on a 3E analysis", *Energy*, **224**, 120135 (2021).
29. Davoodi, V., Kazemiani-Najafabadi, P., and Amiri Rad, E. "Presenting a power and cascade cooling cycle driven using solar energy and natural gas", *Renew. Energy*, **186**, pp. 802–813 (2022).
30. Liu, Z., Liu, Z., Yang, X., et al."Advanced exergy and exergoeconomic analysis of a novel liquid carbon dioxide energy storage system", *Energy Convers. Manag.*, **205**, 112391 (2020).
31. Singh, O.K. and Kaushik, S.C. "Energy and exergy analysis and optimization of Kalina cycle coupled with a coal fired steam power plant", *Appl. Therm. Eng.*, **51**(1–2), pp. 787–800 (2013).
32. Fratzscher, W. "The exergy method of thermal plant analysis", *Int. J. Refrig.*, **20**(5), p. 374 (1997).
33. Bai, T., Yu, J., and Yan, G. "Advanced exergy analyses of an ejector expansion transcritical CO_2 refrigeration system", *Energy Convers. Manag.*, **126**, pp. 850–861 (2016).
34. Kelly, S., Tsatsaronis, G., and Morosuk, T. "Advanced exergetic analysis: Approaches for splitting the exergy destruction into endogenous and exogenous parts", *Energy*, **34**(3), pp. 384–391 (2009).

35. Zhang, Y., Liang, T., Yang, C., et al. "Advanced exergy analysis of an integrated energy storage system based on transcritical CO_2 energy storage and organic rankine cycle", *Energy Convers. Manag.*, **216**, 112938 (2020).
36. Galindo, J., Ruiz, S., and Dolz, V. "Advanced exergy analysis for a bottoming organic rankine cycle coupled to an internal combustion engine", *Energy Convers. Manag.*, **126**, pp. 217–227 (2016).
37. Morosuk, T. and Tsatsaronis, G. "A new approach to the exergy analysis of absorption refrigeration machines", *Energy,* **33**(6), pp. 890–907 (2008).
38. Arslan, O. and Erbas, O. "Investigation on the improvement of the combustion process through hybrid dewatering and air pre-heating process: A case study for a 150 MW coal-fired boiler", *J. Taiwan Inst. Chem. Eng.*, **121**, pp. 229–240 (2021).
39. Wang, Z., Xiong, W., Ting, D.S.K., et al. "Conventional and advanced exergy analyses of an underwater compressed air energy storage system", *Appl. Energy,* **180**, pp. 810–822 (2016).
40. Chen, J., Zhu, K., Huang, Y., et al. "Evaluation of the ejector refrigeration system with environmentally friendly working fluids from energy, conventional exergy and advanced exergy perspectives", *Energy Convers. Manag.*, **148**, pp. 1208–1224 (2017).
41. Bai, T., Yu, J., and Yan, G. "Advanced exergy analysis on a modi fi ed auto-cascade freezer cycle with an ejector", *Energy*, **113**, pp. 385–398 (2016).
42. Hepbasli, A. and Keçebaş, A. "A comparative study on conventional and advanced exergetic analyses of geothermal district heating systems based on actual operational data", *Energy Build.*, **61**, pp. 193–201 (2013).
43. Boyaghchi, F.A. and Molaie, H. "Investigating the effect of duct burner fuel mass flow rate on exergy destruction of a real combined cycle power plant components based on advanced exergy analysis", *Energy Convers. Manag.*, **103**, pp. 827–835 (2015).
44. Dai, B., Zhu, K., Wang, Y., et al. "Evaluation of organic Rankine cycle by using hydrocarbons as working fluids: Advanced exergy and advanced exergoeconomic analyses", *Energy Convers. Manag.*, **197**, 111876 (2019).
45. Çengel, Y. and Boles, M., *Thermodynamics: An Engineering Approach*, Eighth Edi. (2015).
46. Arslan, O. and Acar, M.S. "Enhanced exergetic evaluation of regenerative and recuperative coal-fired power plant", *Int. J. Exergy*, **35**(2), p. 263 (2021).
47. Fallah, M., S. Mahmoudi, M.S., and Yari, M. "Advanced exergy analysis for an anode gas recirculation solid oxide fuel cell", *Energy*, **141**, pp. 1097–1112 (2017).

Biographies

Mahla Akhoundi received BSc and MSc degrees in Mechanical Engineering from Hakim Sabzevari University, Iran in 2018 and 2021, respectively. She is now a PhD student of Mechanical Engineering at the Department of Mechanical Engineering, Hakim Sabzevari University. Her research interests include analysis of the energy, exergy, and modification of the energy systems.

Parisa Kazemiani-Najafabadi is a Doctor of Mechanical Engineering at the Department of Mechanical Engineering, Hakim Sabzevari University. Her research field is modeling energy systems, especially power and cooling systems. According to the research field, she has published over 10 papers in top journals.

Ehsan Amiri Rad has been an Associate Professor at the Department of Mechanical Engineering, Hakim Sabzevari University, Iran since June 2013. His main teaching contribution has been to undergraduates in engineering thermodynamic and to postgraduate students in exergy. He is currently involved in energy optimization for power and cooling systems and has already carried out several projects. He has published over 40 papers in different journals.